Title: Pre- and post-target cortical processes predict speech-in-noise performance

Abbreviated title: Neural correlates of speech-in-noise performance

Subong Kim,[1, #] Adam T. Schwalje,[2, #] Andrew S. Liu,[2] Phillip E. Gander,[3] Bob McMurray, [1,2,4] Timothy D. Griffiths,[5] and Inyong Choi[1, 2, *]

[1] Department of Communication Sciences and Disorders, University of Iowa, Iowa City, IA 52242, USA

[2] Department of Otolaryngology – Head and Neck Surgery, University of Iowa Hospitals and Clinics, Iowa City, IA 52242, USA

[3] Department of Neurosurgery, University of Iowa Hospitals and Clinics, Iowa City, IA 52242, USA

[4] Department of Psychological and Brain Sciences, University of Iowa, Iowa City, IA 52242, USA

[5] Biosciences Institute, Newcastle University, Newcastle upon Tyne, NE1 7RU, UK

[#] SK and ATS contributed equally to this work.

[*] Corresponding author at: Department of Communication Sciences and Disorders, University of Iowa, 250 Hawkins Dr., Iowa City, IA 52242, USA. Email address: inyong-choi@uiowa.edu

Author contributions:

S.K. and A.T.S. contributed equally to this work. I.C. designed the experiments. S.K. ran the experiments. S.K., A.T.S., A.S.L., P.E.G., B.M., T.D.G., and I.C. analyzed and interpreted data. S.K., A.T.S., and I.C. prepared the manuscript, with revisions and suggestions from A.S.L, P.E.G., B.M., and T.D.G..

Abstract

Understanding speech in noise (SiN) is a complex task that recruits multiple cortical subsystems. There is a variance in individuals' ability to understand SiN that cannot be explained by simple hearing profiles, which suggests that central factors may underlie the variance in SiN ability. Here, we elucidated a few cortical functions involved during a SiN task and their contributions to individual variance using both within- and across-subject approaches. Through our within-subject analysis of source-localized electroencephalography, we investigated how acoustic signal-to-noise ratio (SNR) alters cortical evoked responses to a target word across the speech recognition areas, finding stronger responses in left supramarginal gyrus (SMG, BA40 the *dorsal lexicon* area) with quieter noise. Through an individual differences approach, we found that listeners show different neural sensitivity to the background noise and target speech, reflected in the amplitude ratio of earlier auditory-cortical responses to speech and noise, named as an *internal SNR*. Listeners with better *internal SNR* showed better SiN performance. Further, we found that the post-speech time SMG activity explains a further amount of variance in SiN performance that is not accounted for by *internal SNR*. This result demonstrates that at least two cortical processes contribute to SiN performance independently: pre-target time processing to attenuate neural representation of background noise and post-target time processing to extract information from speech sounds.

Keywords

Speech-in-noise, speech unmasking, speech recognition, individual differences, electroencephalography, supramarginal gyrus

1. Introduction

Understanding speech in noise (SiN) is essential for communication in social settings. Young normal-hearing listeners are remarkably adept at this. Even in challenging SiN conditions where the speech and noise have the same intensity (i.e., 0 dB signal-to-noise ratio: SNR) and overlapped frequency components, they often recognize nearly 90% of sentences correctly (Ohlenforst et al., 2017). This suggests a surprising capacity of the auditory system to cope with noise. However, the ability to understand SiN degrades severely with increased background noise level (Ohlenforst et al., 2017), hearing loss (Harris and Swenson, 1990), and/or aging (Nabelek, 1988).

Recent studies show that normal hearing listeners show large individual differences in SiN performance (Liberman et al., 2016). The premise of this study is that by linking this variable ability for SiN perception to variation in cortical activity, we may be able to understand the neural mechanisms by which humans accomplish this ability, and this may shape our understanding of how best to remediate hearing loss.

Two broad neural mechanisms might give rise to better or worse SiN performance. First, listeners may vary in neural processing that separates the target auditory object from the mixture of sounds (i.e., similar to *external* selection processes in (Strauss and Francis, 2017). Auditory scene analysis (Bregman, 1999) processes, when occurring in parallel with auditory selective attention (Shinn-Cunningham, 2020), can inhibit the neural representation of competing sounds and enhance the neural response to attended input. This process has been conceptualized as a form of sensory gain control (Hillyard et al., 1998) or neural filtering (Obleser and Erb, 2020). Its effectiveness is often quantified as attentional modulation index (AMI), the amplitude ratio of evoked responses to background noise and target (Dai and Shinn-Cunningham, 2016; O'Sullivan et al., 2019), or the degree of neural phase-locking to the attended speech (Etard and Reichenbach, 2019; Mesgarani and Chang, 2012; Viswanathan et al., 2019). A successful sensory gain control, indicated by a positive AMI, during a SiN task will

unmask the target speech from maskers, which will enhance the effective signal-to-noise ratio (SNR) in the central auditory pathway (e.g., the primary and secondary auditory cortices in the superior temporal plane: STP and the posterior superior temporal gyrus: STG).

Second, listeners might vary in neural processes for the prompt extraction of information from a speech signal (i.e., similar to *internal* selection processes in (Strauss and Francis, 2017). An inherent challenge in recognizing speech (e.g., a spoken word) is the mapping between the incoming speech cues and higher level units like words and meaning while speech unfolds rapidly over time [for review, see Weber and Scharenborg (2012), Dahan and Magnuson (2006), and Davis (2016) with references therein]. In quiet listening conditions, average young normal-hearing listeners activate a range of lexical candidates immediately at the onset of the auditory stimulus (i.e., shown by works using eye-movements in the visual world paradigm: (Allopenna et al., 1998; Dahan and Gareth Gaskell, 2007; Magnuson et al., 2007). For example, after hearing the /ba/ at the onset of *bakery*, listeners will immediately consider a range of words like *bacon*, *bathe,* or *base*, at both phonological and semantic levels. However, such rapid lexical processing develops slowly in children (Rigler et al., 2015); continuous differences in lexical processing are linked to differences in language ability (McMurray et al., 2010); and they differ in listeners with hearing loss or deteriorated acoustic-cue encoding (McMurray et al., 2019). These facts suggest that there can be individual differences in the prompt lexical processing even for *clean* speech signals.

It is as yet unclear the degree to which variation in SiN performance is related to variation in both processes (particularly in combination).

Assessing Individual Differences in Speech Unmasking. Individual differences in the speech unmasking pathway may arise from 1) the fidelity of encoding supra-threshold acoustic features and 2) cognitive control of the domain-general attentional network. Auditory scene analysis relies on the supra-threshold acoustic features that provide binding cues for auditory grouping (Darwin, 1997). These include the spectra (Lee et al., 2013), location (Frey et al.,

2014; Goldberg et al., 2014), temporal coherence (Moore, 1990; Shamma et al., 2013; Teki et al., 2011), rhythm (Calderone et al., 2014; Golumbic et al., 2013; Herrmann et al., 2016; Obleser and Kayser, 2019), and timing (Lange, 2009) of the figure and ground. The fidelity of encoding such supra-threshold acoustic features may affect the separation of target speech from background noise. Supporting this idea, previous studies have correlated the fidelity of supra-threshold acoustic cue coding to SiN understanding (Anderson and Kraus, 2010; Anderson et al., 2013; Holmes and Griffiths, 2019; Hornickel et al., 2009; Liberman et al., 2016; Parbery-Clark et al., 2009; Song et al., 2011).

Individual differences also exist in how strongly selective attention modulates cortical evoked responses to sounds (Choi et al., 2014). This suggests there may be a correlation between top-down selective attention efficacy and SiN performance. Indeed, (Strait and Kraus, 2011) reported that reaction time during a selective attention task predicts SiN performance. Similarly, studies suggest that poor cognitive control of executive attentional network predicts auditory selective attention performance (Bressler et al., 2017; Dai et al., 2018), though this has not been extended to SiN.

We can obtain a measure of the overall function of these bottom-up and top-down neural processing for speech unmasking by quantifying the amplitude ratio of early cortical auditory evoked responses to noise and target speech (similarly to the AMI concept). Here we use the N1/P2 event-related potential (ERP) components which occur with 100-300 ms latency. Previous studies showed that such ERP components are strongly modulated by selective attention but only when auditory objects are successfully segregated (Choi et al., 2013; Choi et al., 2014; Kong et al., 2015). Since those early cortical ERP components originate from multiple regions across Heschl's gyrus (i.e., the primary auditory cortex) and its surrounding areas (e.g., posterior superior temporal gyrus) (C□eponien et al., 1998), an efficient and collective way of indexing the neural efficiency in speech unmasking is using a scalp electroencephalographical (EEG) potential at the vertex [e.g., "Cz" of the international 10-10 system for EEG electrode

125 montage: Koessler et al. (2009) within a limited time-window (e.g., 100-300 ms range after the
126 stimulus onset].

127 ***Assessing Individual Differences in Mapping Speech to Words and Meaning.*** To
128 assess individual differences related to the second neural mechanism – the downstream speech
129 information processing – we must assess a larger range of cortical regions above the auditory
130 brainstem and cortex. Current models of speech processing suggest two distinct cortical
131 networks (i.e., dorsal and ventral stream) that are used in parallel (Gow, 2012; Hickok and
132 Poeppel, 2007; Myers et al., 2009; Scott and Johnsrude, 2003). The ventral stream pathway
133 including anterior superior temporal and middle temporal gyri (STG/MTG) integrates speech-
134 acoustic and semantic information progressively over time for the sound-to-meaning mapping
135 (Davis and Johnsrude, 2003). The dorsal stream pathway comprising supramarginal gyrus
136 (SMG, also known as tempo-parietal junction or TPJ) and pre- / post-central gyri mediates the
137 mapping between sound and articulation (Rauschecker and Scott, 2009), while inferior frontal
138 gyrus (IFG) interacts with both pathways for lexical decision-making processes (Gow, 2012).

139 Studies have compared cortical responses in these areas to spoken words against
140 acoustically-matching non-word sounds. These highlight the SMG/TPJ, MTG, and IFG in the
141 left hemisphere as three regions that tend to exhibit more activity for words than pseudo-words
142 (Davis and Gaskell, 2009; Taylor et al., 2013). The dual lexicon model suggested by Gow
143 (2012) confirms the importance of those three regions by referring to left SMG and MTG as
144 dorsal and ventral lexicons that communicate with left IFG for lexical decision making. While
145 both SMG and MTG exhibit explicitly lexical representations, they may take complementary
146 roles consistent with the dual stream pathway model (Gow, 2012; Hickok and Poeppel, 2007).
147 Thus, the type of task (e.g., whether subjects are asked to make a phonological or semantic
148 judgment) may influence the relative dominance between SMG and MTG activities during
149 speech recognition.

Supporting the idea of broad cortical regions contributing to individual differences in speech processing, fMRI studies showed that SNR changes alter the level of neural activities across frontal, central, and temporo-parietal regions (Du et al., 2016; Vaden et al., 2015; Wong et al., 2009; Zekveld et al., 2006), while Du et al. (2016) reported the correlation between activities in fronto-central regions and speech recognition performance. However, these correlations could reflect earlier variation in speech unmasking – if auditory/attentional unmasking mechanisms are less efficient, then they could lead to differences in how strongly later regions (IFG, SMG, etc.) must work to recognize words or complete the task. Thus, it is crucial to evaluate both mechanisms simultaneously to isolate a potential role for later processes.

In addition to testing the loci of activities, it is also important to test the relative timing of activity in these pathways during speech processing. Functionally, studies using eye-movements in the Visual World Paradigm (VWP) have extensively characterized the time course of word recognition in both quiet (Allopenna et al., 1998; Dahan and Gareth Gaskell, 2007; Magnuson et al., 2007) and under challenging conditions such as noise or signal degradation (Ben-David et al., 2011; Brouwer and Bradlow, 2016; Huettig and Altmann, 2005; McMurray et al., 2017; McQueen and Huettig, 2012). Most VWP data show that, in quiet, the maximum lexical competition occurs at ~400 ms after the onset. These studies also report delayed processing under challenging conditions, but such delays do not exceed 250 ms even under the most severe degradation. This timing information can guide us when we interpret the functional implication of neural activity within certain regions; if the latency of neural activity is larger than ~400 ms, such activity may be less likely related to the online word recognition.

However, the timing of cortical activity within each pathway and the way this may be moderated by challenging listening conditions are largely unknown. This is true both within isolated regions (e.g., SMG or MTG) and across activation of broader regions (e.g., frontal lobe). This is because most of the work on speech in noise perception has been conducted with

fMRI (Du et al., 2014, 2016; Wong et al., 2009; Wong et al., 2008) which has a poor temporal resolution. One study has examined evoked responses across speech processing regions using source localized EEG (Bidelman and Howell, 2016). This suggests an early response at roughly 100 ms post-stimulus in IFG. However, this study used non-sense syllables that cannot reveal lexical processes.

The present study. The central aim of this study is to investigate the simultaneous contributions of both speech unmasking and speech recognition processes to the individual differences in SiN understanding. Our main question is whether the early-stage speech *unmasking* and later-stage *recognition* processes independently predict SiN performance, or whether the latter variable is dependent on the former. We attempted to answer this question through the combination of within- and across-subject analyses using both sensor- and source-space evoked responses in an EEG paradigm.

Subjects performed a SiN noise task in which they heard isolated consonant-vowel-consonant (CVC) English words and selected which of four orthographically presented words matched the auditory stimuli. Noise began 1 second before the speech. Two noise conditions were used: a low SNR (-3 dB) or hard condition, and high SNR (+3 dB) or easy condition. EEG was recorded from 64 electrodes while subjects performed this task, using both source- and sensor-space analyses to quantify cortical activity.

Speech unmasking and speech recognition can be distinguished by the 1) timing and 2) regional differences of neural activities evoked by both noise and target speech. Thus, we used a trial structure comprised of clearly separated events (i.e., fixed onsets of background noise and target speech) while observing time-locked neural responses to such events with electroencephalography (EEG). The degree of speech unmasking was quantified as the amplitude ratio of evoked responses to the onsets of noise and target speech measured at a vertex scalp electrode (the key scalp location for evoked responses from early auditory processes), henceforth referred to as *internal SNR*. Although the concept of *internal SNR* is

similar to the attentional modulation index (Dai and Shinn-Cunningham, 2016; O'Sullivan et al., 2019), we named the index rather phenomenologically to avoid limiting the mechanism underlying the index to selective attention.

The effectiveness of later speech *recognition* processing was quantified by measuring the amplitude of evoked responses within target cortical regions. As we described, prior work has implicated a number of such regions. However, it is unclear which may be relevant for our specific task. Thus, we take a data-driven approach by first asking which post-auditory regions show *greater* activity in the *higher* SNR (easier) listening condition. This would be suggestive of a region that conducts downstream analyses once the target speech is unmasked. We looked into two regions-of-interest (ROIs): left SMG and IFG. As reviewed above, those regions activate more strongly for speech than pseudo-speech sounds; we did not consider MTG (the ventral lexicon) as our task was single CVC word identification (matched to an orthographic response). In this task, phonological discrimination (indicating the dorsal stream), rather than semantic processing, is essential.

Having quantified the contributions of each pathway, we then conducted both timing and individual differences analyses to determine their relative contribution to SiN performance.

2. Material and Methods

2.1 Participants

Twenty-six subjects between 19 and 31 years of age (mean = 22.42 years, SD = 2.97 years; median = 21.5 years; 8 (31%) male) were recruited from a population of students at the University of Iowa. All subjects were native speakers of American English, with normal hearing thresholds no worse than 20 dB HL at any frequency, tested in octaves from 250 to 8000 Hz. Written informed consent was obtained, and all work has been carried out in accordance with the Code of Ethics of the World Medical Association (Declaration of Helsinki). All study procedures were reviewed and approved by the University of Iowa Institutional Review Board.

2.2 Task design and procedures

We aimed to simultaneously measure SiN performance and cortical neural activity in a short (15 minute) experimental session. Sessions were kept short to avoid confounding individual differences in irrelevant psychological factors – fatigue, level or engagement –with individual differences in performance and processing.

Each trial (**Figure 1**) began with the presentation of a fixation cross ('+') on the screen. Listeners were asked to fix their gaze on this throughout the trial to minimize eye-movement artifacts. Next, they heard the cue phrase "check the word." This enabled listeners to predict the timing of next acoustic event (the noise onset). After a 700 ms of silence, the multi-talker babble noise began and continued for 2 seconds. One second after the noise onset, the target word was heard. Finally, 100 ms after the composite auditory stimulus (noise + word) offset, four written choices appeared on the screen. The response options differed either in the initial or the final consonant (e.g., for target word *ban*, options were *than*, *van*, *ban*, and *pan;* for target word *hiss,* options included *hit*, *hip*, *hiss*, *hitch*). Subjects pressed a button on a keypad to indicate their choice and no feedback was given. The next trial began 1 second after the button press.

This trial structure was intended to minimize visual, pre-motor, and motor artifacts during the time of interest surrounding the auditory stimuli. The timing and intervals of auditory stimuli (i.e., cue phrase, noise, and target) were intended to derive well-distinct cortical evoked responses to the onsets of background noise and target word.

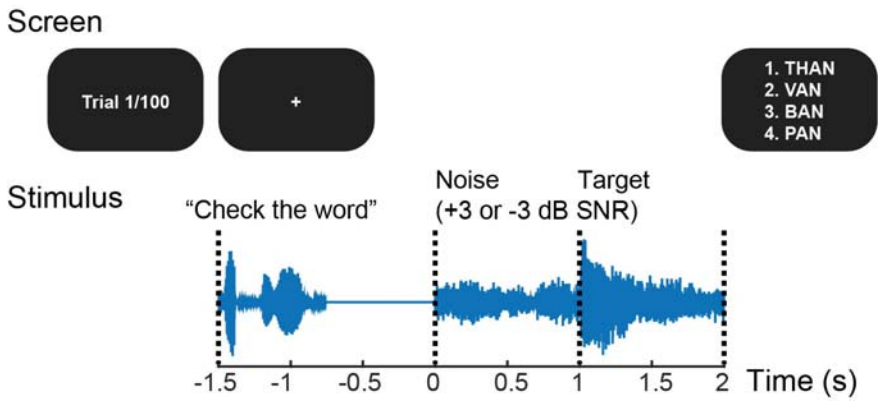

Figure 1. Trial and stimulus structure. Every trial starts with the cue phrase "check the word." A target word starts 1 second after the noise onset. Four choices are given after the word ends; subjects select the correct answer with a keypad. No feedback is given. The noise level is manipulated to create high (+3 dB) and low (-3 dB) SNR conditions. Subjects complete 50 trials for each condition.

Since we were particularly interested in SMG and IFG regions that are involved in phonological and lexical processing (Gow, 2012; Hickok and Poeppel, 2007), we used naturally spoken words, rather than non-sense speech tokens used by prior EEG studies (Bidelman and Howell, 2016; Parbery-Clark et al., 2009). Target words consisted of hundred monosyllabic CVC words from the California Consonant Test (CCT) (Owens and Schubert, 1977), spoken by a male speaker with a General American accent.

Target words were always presented at 65 dB SPL. In each trial, the RMS level of noise was chosen randomly between 68 and 62 dB SPL to yield either -3 or +3dB SNR (referred to as "low SNR" and "high SNR," respectively). Fifty words were presented at each SNR. -3 dB SNR was chosen from pilot experiments to emulate a condition yielding a mid-point performance (~65% correct) in the possible accuracy range (i.e., 25 – 100%), at which listening effort and individual differences in performance may be maximized (Ohlenforst et al., 2017). Thus, the SiN performance at -3 dB SNR condition was used for the later correlational analysis in this study. +3 dB SNR was chosen to emulate a less noisy condition from which the downstream speech recognition process will be measured for the correlational analysis.

The task was implemented using the Psychtoolbox 3 package (Brainard, 1997; Pelli, 1997) for Matlab (R2016b, The Mathworks). Participants were tested a sound-treated, electrically shielded booth with a single loudspeaker (model #LOFT40, JBL) positioned at a 0° azimuth angle at a distance of 1.2 m. A computer monitor was located 0.5m in front of the subject at eye level. The auditory stimuli were presented at the same levels for all subjects.

2.3 EEG acquisition and preprocessing

Scalp electrical activity (EEG) was recorded during the SiN task using the BioSemi ActiveTwo system at a 2048 Hz sampling rate. Sixty-four active electrodes were placed according to the international 10-20 configuration. Trigger signals were sent from Matlab (R2016b, The Mathworks) to the ActiView acquisition software (BioSemi). The recorded EEG data from each channel were bandpass filtered from 1 to 50 Hz using a 2048-point FIR filter. Epochs were extracted from -500 ms to 3 s relative to stimulus onset. After baseline correction using the average voltage between -200 and 0 ms, epochs were down-sampled to 256 Hz.

Since we were interested in the speech-evoked responses from frontal brain regions, we opted for a non-modifying approach to eye blink rejection: Trials that were contaminated by an eye blink artifact were rejected based on the voltage value of the Fp1 electrode (bandpass filtered between 1 and 20 Hz). Rejection thresholds for eye blink artifacts were chosen individually for each subject, and separately for the noise and target word periods. After rejecting bad trials, averages for each electrode were calculated for the two conditions to extract evoked potentials. For analysis of speech-evoked responses, we repeated baseline correction using the average signal in the 300 ms preceding the word onset.

2.4 Sensor-space analysis

We performed traditional sensor-space ERP analysis to investigate the effect of acoustic SNR on AC representation of noise and speech, and its individual differences. The other

purpose of sensor-space analysis was to ensure the quality of data in the more familiar form before running source-space analyses.

Cortical evoked responses time-locked to the target and noise were examined and compared between high- and low-SNR conditions. EEG data were bandpass filtered from 2 to 7 Hz to capture auditory N1 and P2 components that fall into 3 – 5 Hz bands. Our first, analysis examined the N1 and P2 peak amplitude obtained from the frontal-central channels (C1, C2, FC1, FC2, FCz, Cz) and compared these measures between two SNR conditions. Both auditory N1 and P2 components were obtained at around 200 ms after the noise onset and at about 250 ms after the target word onset. After comparing the amplitude of each auditory component, we also examined the ERP envelopes by applying the Hilbert transform to the bandpass-filtered ERPs and taking the absolute value to effectively represent overall magnitude of both N1 and P2 ERP components. Then, "internal SNR" was defined as the ratio of target word-evoked ERP envelope peaks to noise-evoked ERP envelope peaks magnitude in dB scale (Equation 1). We computed this index expecting to quantify a "neural" form of an individual's speech unmasking ability. The internal SNR is different for each subject, and is separate from the fixed external, or acoustic, SNR (here, ±3 dB).

$$\text{(1)}\quad Internal\ SNR = 20log_{10}\frac{\text{Target–evoked potential}}{\text{Noise–evoked potential}}$$

Mean activity levels were jackknifed prior to testing to assess the variance with clean ERP waveforms. In this approach, the relevant neural factors were computed for all subjects but one. This was repeated leaving out each subject in turn. The resulting statistics were adjusted for jackknifing to reflect the fact that each data point reflects N-1 subjects (Luck, 2014).

2.5 Source analysis

The source-space analysis was based on minimum norm estimation (Gramfort et al., 2013; Gramfort et al., 2014) as a form of multiple sparse priors (Friston et al., 2008). After co-registration of average electrode positions to the reconstructed average head model MRI, the forward solution (a linear operator that transforms source-space signals to sensor space) was computed using a single-compartment boundary-element model (Hämäläinen, 1989). The cortical current distribution was estimated assuming that the orientation of the source is perpendicular to the cortical mesh. Cross-channel EEG-noise covariance, computed for each subject, was used to calculate the inverse operators. A noise-normalization procedure was used to obtain dynamic statistical parametric maps (dSPMs) as *z*-scores (Dale et al., 2000). The inverse solution estimated the source-space time courses of event-related activity at each of 10,242 cortical voxels per hemisphere.

Following the whole-brain source estimation, we extracted representative source time courses from regions of interests (ROIs). In the present study, two predetermined ROIs were used: (1) left SMG, and (2) left pars opercularis and pars triangularis of IFG. Destrieux Atlas of cortical parcellation (Fischl et al., 2004) was used to predetermine ROIs anatomically.

Since we did not have individual structural MRI head models, it was not ideal to take the summed activity (mean or median) for all the voxels within ROIs. This is because individual difference in functional and anatomical structure of the brain may result in spatial blurring since current densities across adjacent voxels can overlap each other. Instead, representative voxels were identified for each ROI, for each SNR condition. We used a combination of previously-described methods to select voxels of interest that were used in fMRI studies (Tong et al., 2016). The voxel selection was performed by a two-step process. First, we selected voxels that exhibit greater-than-median amplitude in either (high ***or*** low SNR condition) condition. Second, cross-correlation coefficients for ERP time courses across all remaining voxels in an ROI were calculated across time, and then the mean coefficient was calculated for each voxel. The most representative voxel was defined as having the maximum mean correlation coefficient, while

346 also being above threshold at two or more continuous timepoints based on voxel's *p*-value, as
347 determined using one-sample *t*-tests (Tong et al., 2016).
348 For the downstream statistical analyses, temporal envelopes were extracted from the
349 within-ROI source time courses. The source time course envelopes at different ROIs were
350 based on slightly different frequency ranges: 2-7 Hz for SMG and 1-5 Hz for IFG. This was to
351 reflect the differences between temporal and frontal lobes in their dominant neural oscillations
352 which create evoked activities through phase coherence (Giraud and Poeppel, 2012).
353
354 ***2.6 Statistical approaches***
355 Once the temporal envelope of the source time course from the most representative
356 voxel was obtained for each SNR condition, mean activity levels were compared between the
357 two SNR conditions using paired *t*-tests. Here, we also used a jackknifing approach, and test
358 statistics were adjusted to account for the fact that each data-point represents N-1 participants.
359 Finally, to identify timepoints that showed a significant difference between SNR conditions while
360 addressing multiple comparison problem, the cluster-based permutation tests were conducted
361 (Maris and Oostenveld, 2007).
362 In order to identify predictors of SiN performance, sensor and source space indices of
363 activity were used in correlation/regression analysis with SiN performance (accuracy) as the
364 dependent variable, and the peak magnitudes of the ERP envelopes from ROIs, and internal
365 SNR as the predictor variables. The peak magnitudes of the ERP envelopes were obtained over
366 timepoints that showed a significant difference between high and low SNR conditions identified
367 in the ROI-based source analysis described above. After calculating the correlation between
368 SiN performance and these predictors, a joint contribution was tested using linear regression
369 analysis to simultaneously examine bottom-up and compensatory related SiN performance to
370 three factors.
371

3. Results

Our analysis started by examining the effect of SNR on task performance (accuracy and reaction time). This was intended to document that noise manipulation had the expected effect. Next, we examined the effect of SNR on both the magnitude and timing of neural activity. This was done first in the sensor-space, using the auditory N1/P2 components and other measures to examine primary auditory pathways. Next, this was done in the source-space to examine the compensatory role of IFG, to evaluate whether IFG effects were early enough to play a role in speech perception, and to test hypotheses about SMG. Finally, we turn to our primary analysis: a regression testing the unique contributions of each pathway to individual differences in SiN performance. Original raw and processed data of the present study are available at Mendeley Data (http://dx.doi.org/10.17632/jyvythkz5y.1).

3.1 SiN performance

There was a large variance in performance among participants. This was observed in both the high SNR condition (accuracy: mean = 80.64%, SD = 7.81%, median = 83.01%; reaction time: mean = 1.53 s, SD = 0.32 s, median = 1.55 s) and the low SNR condition (accuracy: mean = 68.21%, SD = 8.92%, median = 70.37%; reaction time: mean = 1.70 s, SD = 0.36 s, median = 1.69 s). There was a significant effect of SNR on both accuracy ($t(25) = 6.99$, $p < 0.001$, paired t-test) and reaction time ($t(25) = -3.81$, $p < 0.001$, paired t-test) (**Figure 2A**). Reaction time and accuracy were correlated in the high SNR condition (**Figure 2B**, $r = -0.50$, $p = 0.009$), but not in the low SNR condition (**Figure 2C**, $r = -0.19$, $p = 0.34$).

As a whole, these results validate that the SNR manipulation was sufficient to create differences in speech perception. The negative correlation between the accuracy and reaction

time may demonstrate the redundancy between individual differences of accuracy and difficulty.

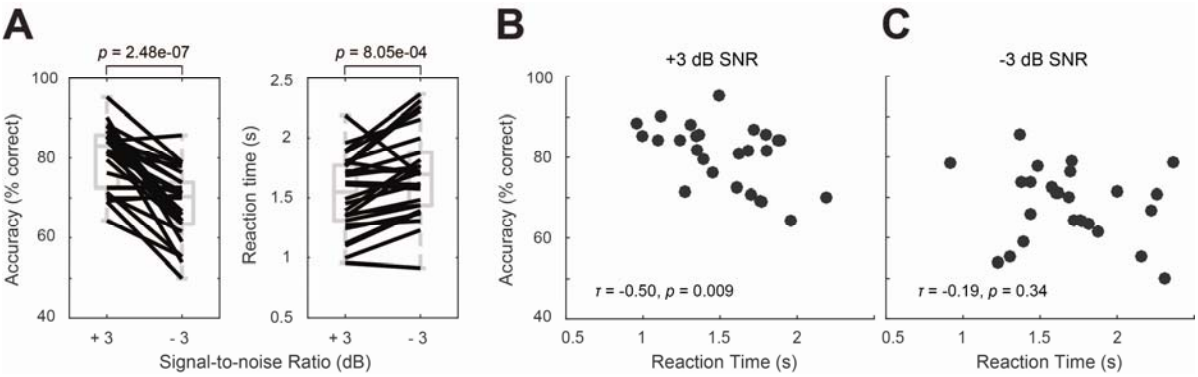

Figure 2. Behavioral results. **A.** Summary of behavioral performance for the two conditions (+3 and -3 dB SNR). Boxes denote the 25th – 75th percentile range; the horizontal bars in the center denote the median; the ranges are indicated by vertical dashed lines. Solid lines connect points for the same subject in different conditions. **B.** Average accuracy as a function of reaction time in +3 dB SNR condition. **C.** Average accuracy and reaction time in -3 dB SNR condition.

3.2 Auditory N1-P2 components in the sensor space

We next examined the N1 and P2 peak amplitude for both noise- and target word-evoked responses. This was done to estimate the contribution of primary auditory pathways and the effect of noise. These measured were compared between high- and low-SNR conditions.

We started with the noise-evoked responses (i.e., peak ERP components arising ~0.2 seconds following the noise onset at 0 s). Here, both N1 ($t(25)$ = -2.64, p = 0.014) and P2 amplitudes ($t(25)$ = -3.82, p < 0.001) were greater in the low SNR condition. In contrast, target-word evoked responses (i.e., peak ERP components arising ~0.25 seconds following the target-word onset at 1 s) showed the opposite pattern with stronger N1 ($t(25)$ = 1.87, p = 0.073) and P2 amplitude ($t(25)$ = 2.41, p = 0.023) in the high-SNR condition (**Figure 3**).

We also examined the ERP envelopes in the time region of both the auditory N1 and P2. Again in the noise-evoked time region, we saw a greater response in the low SNR condition ($t(25)$ = -3.95, p < 0.001). However, also as in the N1/P2 analysis we saw larger word-evoked response in the high SNR condition ($t(25)$ = 2.37, p = 0.026) (**Figure 3**). Then we calculated the internal SNR, the magnitude ratio of the noise and target-word related ERP envelopes, and saw a greater internal SNR in the high SNR condition ($t(25)$ = 2.53, p = 0.018).

The topographical layout of these effects is shown in **Figure 3** (top panels) at the time of the peak P2 (which showed a significant overall effect of noise level) for both noise- and word-evoked response. T-values from paired t-tests on peak P2 amplitudes at all electrodes between SNR conditions were also represented in topographies. These show a broad-based effect that is roughly centered at frontal-central channels for both the noise onset and speech onset (though patterns for the speech evoked P2 were more distributed along the scalp). This justifies our use of frontal-central channels for sensor-space analyses. The significant difference in auditory ERP envelopes and in the N1/P2 components according to the noise level supports our use of the internal SNR as an index of individual ability to modulate representations of target speech relative to noise in the regression analysis.

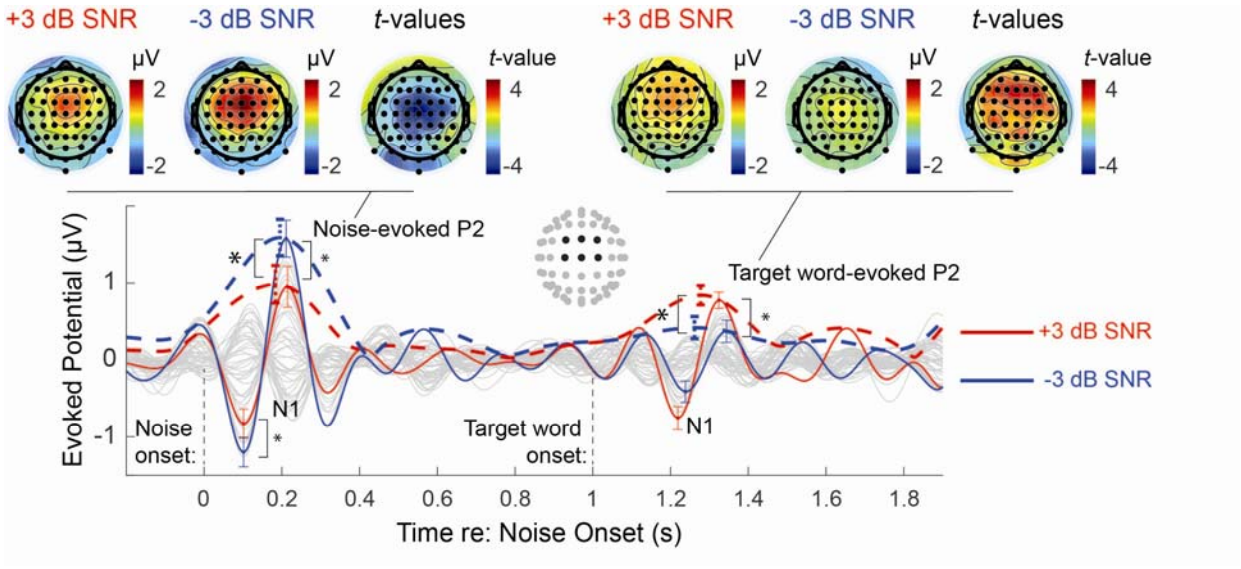

Figure 3. Sensor-level event-related potential (ERP) with the topographical layout and cortical maps. The time course of the auditory ERP and its envelope, with the standard error of the mean (±1 SEM) at the peak amplitude (red color: +3 dB SNR, blue color: -3 dB SNR). An asterisk shows a significant difference in the amplitude between +3 and -3 dB SNR conditions (paired *t*-test). Top panels show peak P2 amplitudes of all electrodes in topographical layouts. The *t*-values from paired *t*-tests between two SNR conditions are also shown as topographies.

3.3 The effect of SNR on cortical activity

Next, we conducted parallel analyses in source space to assess cortical activity through speech processing regions. We converted sensor-space EEG signals to whole-brain source

time courses to localize the effects of SNR on evoked responses within targeted ROIs. Within left SMG, the cluster-based permutation test (Maris and Oostenveld, 2007) revealed that the high SNR condition evokes significantly greater activity than the low SNR condition from 270 to 340 ms (p = 0.0020) (**Figure 4A left**). High-SNR peak amplitude is found at 309 ms. Such a significant SNR effect was not found in the left IFG. The maximum magnitude of the grand average low-SNR evoked response (dSPM) is at 770 ms (**Figure 4B left**). Source time courses in the right SMG and IFG are shown in **Figure 4A and B** (the right panels) for visual comparisons.

Single time-point evoked-current estimates are shown for the peak SMG activity time (i.e., 309ms, **Figure 4C**) and IFG peak time (770ms, **Figure 4D**) on the whole left-hemisphere cortical surface. At 309ms, post-hoc paired *t*-tests on all the left-hemisphere voxels reveal an area near left SMG that shows greater evoked responses in the high SNR condition. This supports a significant role for SMG in SiN processing in this task. In contrast, at 770ms, no voxel was found within IFG that shows significant differences between high- vs. low-SNR conditions. This confirms our timecourse analyses of IFG, suggesting it does not play a large role and that the trend that was observed is not broadly seen across voxels.

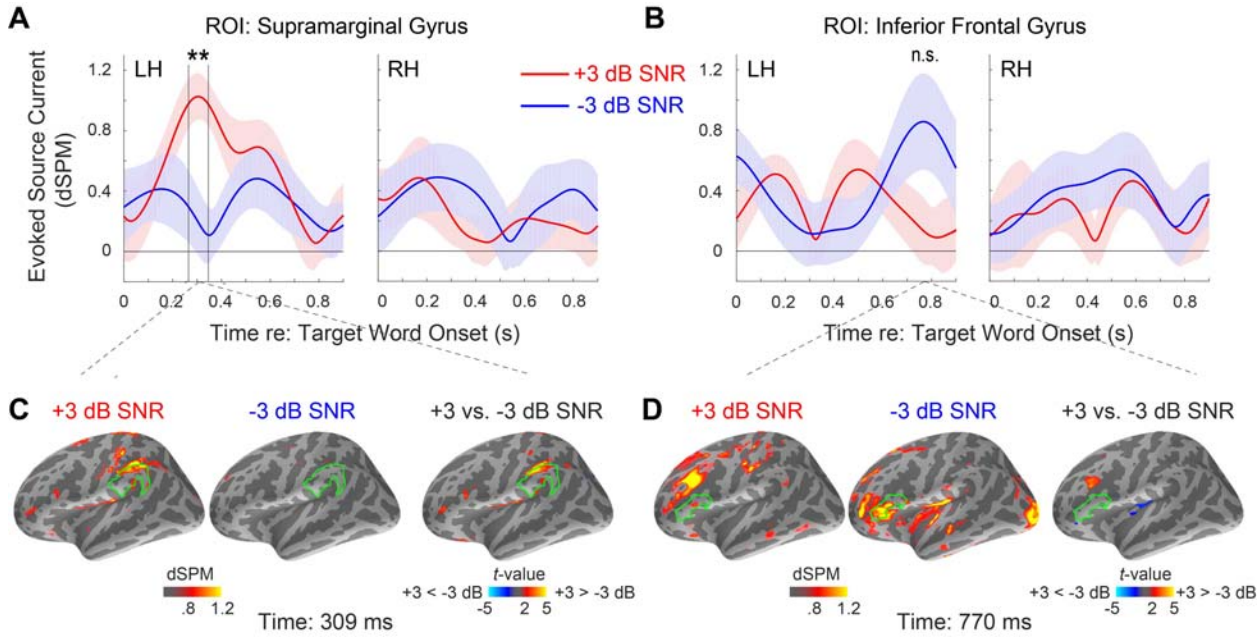

Figure 4. Region-of-interest (ROI) based source analysis. **A and B.** The time course of the event-related potential (ERP) envelope, with the standard error of the mean (±1 SEM), obtained at representative voxels for two ROIs in the left hemisphere ("LH"): supramarginal gyrus (SMG), and the pars opercularis and triangularis of the inferior frontal gyrus (IFG), respectively, in each SNR condition (red color: +3 dB SNR, blue color: -3 dB SNR). The ERP envelope time courses in the corresponding regions in the right hemisphere ("RH") are also shown for visual comparisons. Asterisks show the timing of a significant difference between +3 and -3 dB SNR conditions (cluster-based permutation test, $p = 0.0020$) at the left SMG. **C and D.** Whole-brain maps showing statistical contrasts (t-values obtained from post-hoc paired t-tests between the two SNR conditions) of source activation at each voxel at the peak timepoint of the grand-average source time course of each ROI.

To demonstrate the timing of SMG activity compared to the timing of phonological events, the webMAUS (Kisler et al., 2017) was used to identify the boundaries between the first and second, and the second and third phonemes in each of the 100 stimuli. A histogram of these acoustic time points is shown in **Figure 5**. This confirms that the peak of evoked activation in SMG (i.e., ~309 ms, denoted by a dashed vertical line) occurs within the time course of target words before the final phoneme is presented.

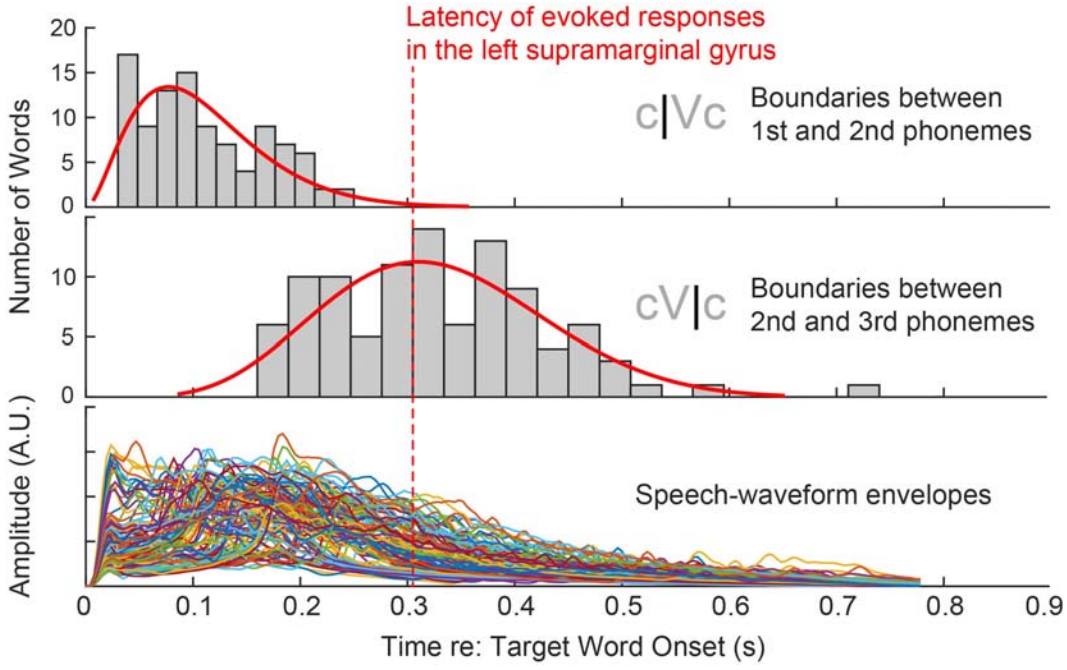

Figure 5. Top and second panel show histograms of boundaries between phonemes of each stimulus. The third panel shows superimposed temporal envelopes extracted from waveforms of the 100 words.

3.4 Individual differences in internal SNR predict SiN performance

To address our primary research question, which was to evaluate the simultaneous contribution of speech unmasking and recognition processes to SiN performance, we conducted a linear regression analysis in which internal SNR and SMG activation were used as independent variables. SiN performance in low SNR condition, which showed larger variance (high SNR SD = 7.81%; low SNR: SD = 8.92%), was used as the dependent variable. We extracted the internal SNR from the low SNR and the SMG activity from the high SNR condition, as we expected that the internal SNR captures how well listeners unmask speech from the noisy background while the SMG activity reflects the processing of relatively clean speech signal. As expected, those two metrics extracted from different trials did not show a correlation (r = -0.04, p = 0.863, the left panel of **Figure 6D**). Both internal SNR ($t(23)$ = 3.35, p = 0.003) and SMG activity ($t(23)$ = 2.29, p = 0.031) were significant predictors of SiN performance (**Figure 6A**). The linear combination of those predictors accounted for a large proportion of the variance (r = 0.64, p = 0.00043, **Figure 6B**).

Figure 6C and D show results from post-hoc correlational analyses. Internal SNR showed a significant correlation with accuracy, while SMG activation did not (despite its significant contribution to the model). There was no correlation between internal SNR and SMG activation, as described above. A semi-partial correlation between SMG activation and the residual of accuracy after regressing out internal SNR was significant, which confirmed that the SMG activation accounted for an extra amount of variance in SiN performance (the right panel of **Figure 6D**). This suggests that in order to identify the contribution of downstream recognition areas like SMG, models must account for the contribution of earlier upstream speech-unmasking processes.

To visualize the contribution of internal SNR to SiN performance, **Figure 6E** showed evoked response differences between good and poor performers (based on a median split on the low-SNR condition accuracy). This reveals dramatic differences in the magnitude of noise onset-related potentials: despite the same physical noise level for each group, good performers

505 exhibited less strong evoked response to noise onset, measured by the envelope peak
506 magnitude within N1-P2 time range in the frontal-central channels (two-sample t-test $t(24) = -2.60$, $p = 0.016$). In contrast, the word-evoked ERP envelope did not show a significant
508 difference between the two groups ($t(24) = 0.21$, $p = 0.84$, two-sample t-test). This suggests that
509 the neural mechanism underlying the internal SNR variance is the suppression of noise (rather
510 than the enhancement of the target).
511

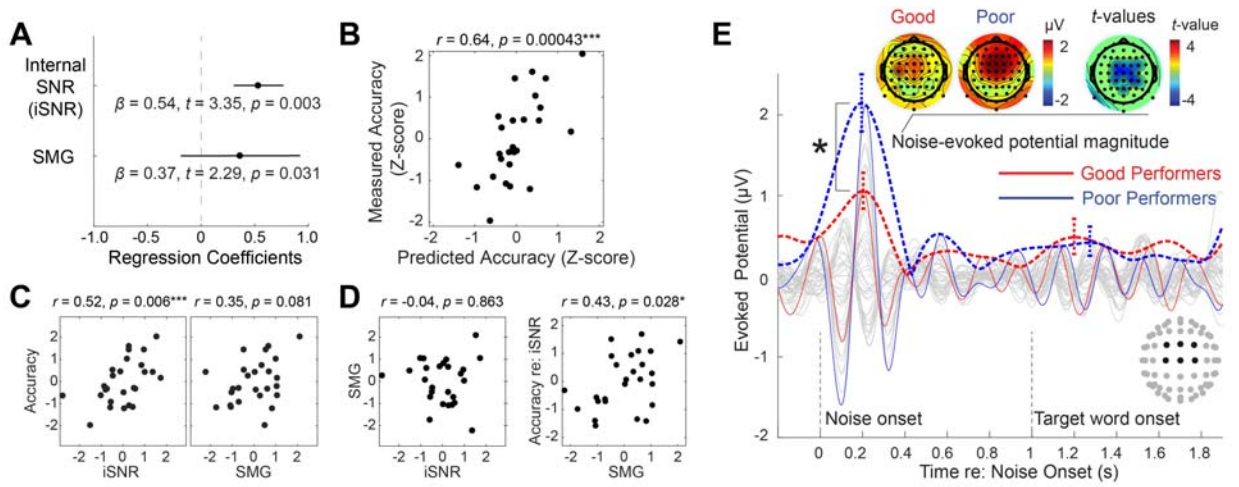

512

513 **Figure 6.** Individual differences in speech-in-noise processing. **A**. Regression coefficients and their
514 standard errors. **B**. A scatter plot showing the relationship between predicted and measured accuracy in -
515 3 dB SNR condition. **C**. Post-hoc correlation analyses: Raw correlations between each independent
516 variable and the dependent variable. **D**. Left: Relationship between independent variables shows no
517 correlation between internal SNR and evoked source current at the left supramarginal gyrus (SMG).
518 Right: Semi-partial correlation between SMG evoked source current and the residual of accuracy after
519 regressing out internal SNR. **E**. The time course of the auditory event-related potential and its envelope,
520 with the standard error of the mean (±1 SEM) at the peak magnitude in -3 dB SNR condition (red color:
521 good performers, blue color: poor performers). An asterisk shows a significant difference in the magnitude
522 between two groups (two-sample *t*-test).
523

524 **4. Discussion**

525 We investigated neural correlates of SiN performance in young normal hearing adults.
526 Previous correlational studies focused on the contributions of either acoustic encoding fidelity
527 (Anderson and Kraus, 2010; Anderson et al., 2013; Holmes and Griffiths, 2019; Hornickel et al.,
528 2009; Liberman et al., 2016; Parbery-Clark et al., 2009; Song et al., 2011) or the degree of

speech/language network recruitment (Du et al., 2016) to the SiN performance. However, the relative importance of each process has remained unclear. We showed that 1) how well the listener suppresses background noise *before* hearing the target speech and 2) how strongly the listener recruits temporo-parietal network *while* the speech signal is received contribute to the SiN performance independently. Combining those two factors explained about 40% of the variance in SiN performance.

Our results have both theoretical and clinical implications. Theoretically, our individual difference approach revealed at least two neural subsystems involve during SiN processing: sensory gain control and post-auditory speech recognition processing. Clinically, our results suggest that a relatively short (~15 minutes) SiN-EEG paradigm can assess crucial neural processes for SiN understanding.

Internal SNR: A measure of pre-speech processing for speech unmasking. The first among the two crucial processes – how well the listener suppresses background noise – was indexed as "internal SNR," the ratio of noise- to target word-evoked cortical responses. This process can be understood as pre-target cortical activity, appearing as an enhanced neural representation of the target sound (the speech) and suppressed neural representation of ignored stimuli (the noise).

What is the source of variation in the internal SNR? Such responses could reflect auditory selective attention, which shows a similar pattern in previous studies (Hillyard et al., 1973; Hillyard et al., 1998; Mesgarani and Chang, 2012). In the present study, good performers showed significantly weaker noise-evoked responses at frontal-central channels (around Cz), compared with poor performers, approximately 200 ms after the noise onset (**Figure 6E**). Decreased auditory responses to background noise in good performers are compatible with the presence of a sensory gain control mechanism (Hillyard et al., 1998) which may happen in multiple sub-regions in STP and posterior STG. The variation in the sensory gain control may originate from multiple factors. It may reflect the acuity of encoding spectro-temporal acoustic

555 cues from speech and noise, or grouping of such acoustic cues for auditory object formation
556 (Moore, 1990; Shamma et al., 2013; Teki et al., 2011). How robustly the low-frequency neural
557 oscillations (e.g., theta and delta) are phase-locked to the acoustic temporal structure of the
558 stimuli (Etard and Reichenbach, 2019) may also contribute to the variation, as the neural phase-
559 locking relies on the encoding of acoustic cues (Ding et al., 2014) and the prediction of temporal
560 structure in speech rhythm (Ding et al., 2016). Since our experiment provided fixed timing of
561 noise and target word onsets, the neural phase-locking based on predicted timing (Arnal and
562 Giraud, 2012) could occur and contribute to the internal SNR. The variation may also reflect
563 endogenous mechanisms for active suppression of background sounds along with neural
564 enhancement of foreground sounds (Shinn-Cunningham and Best, 2008). It was not our goal to
565 disentangle the sources of variation in sensory gain control. Rather, we aimed to quantify the
566 effectiveness of sensory gain control by our unique trial structure that enables clear distinction
567 of evoked responses to noise and target speech, and to test how the internal SNR predicts later
568 speech processes and behavioral accuracy. In this regard, we found a significant correlation
569 between accuracy and the relative magnitude of word- and noise-evoked potentials.

570 ***Evoked amplitude in SMG: the neural marker of effective and prompt lexical***
571 ***processing.*** While the computation of internal SNR was pre-specified, we had an open plan for
572 extracting a representative neural factor to capture post-auditory speech recognition. To explore
573 such neural markers, we added a 6-dB higher SNR condition and asked which region or regions
574 showed increased activity within a reasonable (200 – 500ms) time range. We investigated two
575 ROIs: left SMG and left IFG. As left SMG showed increased evoked response to target speech
576 in the less noisy condition at ~300 ms after the target onset, the peak evoked amplitude in left
577 SMG measured in the high SNR condition was used as the second independent variable in the
578 regression analysis.

579 ***Functional interpretation of SMG activity.*** Previous studies have suggested that
580 spoken-word recognition occurs via a process of dynamic lexical competition as speech unfolds

over time. The VWP studies reported that, for many words, this competition maximizes around 3-400 ms after word onset (Farris-Trimble and McMurray, 2013; Huettig and Altmann, 2005). In significantly challenging conditions (high noise), however, lexical processing can be delayed about 250 ms until most of the word has been heard (Farris-Trimble et al., 2014; McMurray et al., 2017), which may minimize competition. The latency of SMG activity that lied between the second and the third phonemes (see **Figure 5**) in the high SNR condition aligns well with the timing of lexical competition found from the VWP studies, which may suggest that the SMG activity makes a neural substrate of immediate lexical access (Farris-Trimble et al., 2014; McMurray et al., 2017), consistent with Gow (2012). This immediacy was observed when speech sounds were relatively clean (high SNR), and it does not appear in previous EEG studies using non-word synthesized phonemes (Bidelman and Dexter, 2015; Bidelman and Howell, 2016).

After the contribution of speech unmasking (i.e., internal SNR) is regressed out, the SMG evoked amplitude in the cleaner condition predicted the residual of SiN performance (the right panel of **Figure 6D**). This indicates that changes in SMG activity may be an independent factor predicting speech recognition performance, rather than the outcome of pre-speech sensory gain control processing.

Limitation of the current study. In the present paper, we exhibited evoked responses only. Although our results demonstrated how this simple and traditional EEG analysis successfully predicted SiN performance, future studies may pursue further understanding of SiN mechanisms by adopting extended analyses such as induced oscillation (e.g., Choi et al. (2020)) and connectivity analyses.

Our correlational result is limited to young normal hearing listeners where variance does not come from hearing deterioration and aging. This study does not predict how much of the variance can be explained by the combination of internal SNR and SMG activity in the

606 population with larger age ranges. For example, Tune et al. (2020) reported that no correlation
607 is found between neural factors and behavioral success in a large cohort of aged listeners.
608 We chose -3 dB as the main SNR from which the dependent variable for the regression
609 analysis was extracted. Although we claim that the -3 dB SNR provides the most representative
610 condition where the individual difference in performance is maximized, we do not claim that our
611 main findings can be generalized to other SNR conditions.
612 ***Methodological advances and justifications for source time course analysis.*** Our
613 approach to identifying a single voxel within an ROI deserves a particular discussion.
614 Identification of the representative voxel of an ROI is a problem common to EEG source
615 analysis, fMRI, and other functional brain imaging studies. Many relevant neuroimaging analysis
616 approaches have been described, including univariate, multivariate, and machine learning;
617 however, most of these are intended for the identification of regions of interest or functional
618 connections from a whole-brain map. Drawbacks of this type of whole-brain analysis include the
619 need for strict multiple comparisons correction and, therefore, decreased statistical power.
620 Using strong a priori hypotheses to generate regions of interest allowed us to circumvent these
621 issues, but still requires identification of representative voxels within our regions of interest.
622 Favored approaches generally require identification of peak activity within an ROI (Tong et al.,
623 2016). However, to avoid the assumption that choosing peak activity implies, we opted instead
624 to choose the voxel that has the maximum average correlation to every other voxel within the
625 ROI. In the present study, we chose not to constrain the location of the voxel of interest within
626 an ROI for each condition. Because our anatomic resolution is unlikely to be at the voxel level,
627 we elected to choose a different representative voxel for each condition, unconstrained by the
628 location of the representative voxel from other conditions.
629
630 **5. Conclusion**

We found that better speech unmasking in good performers modulated the ratio of cortical evoked responses to the background noise and target sound, which effectively changed SNR internally, resulting in better performance. We also found that clean, intelligible speech elicits early processing at SMG, which explained an extra amount of variance in SiN performance. These findings may collectively form a neural substrate of individual differences in SiN understanding ability; the variance in SiN perception may be a matter of both primary processes that extract the signal from noise and later speech recognition processes to extract lexical information from speech signals promptly.

Acknowledgments

This work was supported by Department of Defense Hearing Restoration and Rehabilitation Program grant awarded to Choi (W81XWH1910637), NIH T32 (5T32DC000040-24) awarded to Schwalje, and NIDCD P50 (DC000242 31) awarded to Griffiths and McMurray. The authors declare no competing financial interests.

References

Allopenna, P.D., Magnuson, J.S., Tanenhaus, M.K., 1998. Tracking the Time Course of Spoken Word Recognition Using Eye Movements: Evidence for Continuous Mapping Models. J Mem Lang 38, 419-439.

Anderson, S., Kraus, N., 2010. Objective Neural Indices of Speech-in-Noise Perception. Trends in Amplification Trends in Amplification 14, 73-83.

Anderson, S., Parbery-Clark, A., White-Schwoch, T., Kraus, N., 2013. Auditory Brainstem Response to Complex Sounds Predicts Self-Reported Speech-in-Noise Performance. Journal of Speech, Language, and Hearing Research 56, 31-43.

Arnal, L.H., Giraud, A.L., 2012. Cortical oscillations and sensory predictions. Trends Cogn Sci 16, 390-398.

Ben-David, B.M., Chambers, C.G., Daneman, M., Pichora-Fuller, M.K., Reingold, E.M., Schneider, B.A., 2011. Effects of aging and noise on real-time spoken word recognition: evidence from eye movements. J Speech Lang Hear Res 54, 243-262.

Bidelman, G.M., Dexter, L., 2015. Bilinguals at the "cocktail party": dissociable neural activity in auditory-linguistic brain regions reveals neurobiological basis for nonnative listeners' speech-in-noise recognition deficits. Brain Lang 143, 32-41.

Bidelman, G.M., Howell, M., 2016. Functional changes in inter- and intra-hemispheric cortical processing underlying degraded speech perception. Neuroimage 124, 581-590.

Brainard, D.H., 1997. The Psychophysics Toolbox. Spat Vis 10, 433-436.

Bregman, A.S., 1999. Auditory scene analysis : the perceptual organization of sound. MIT Press, Cambridge, Mass.

Bressler, S., Goldberg, H., Shinn-Cunningham, B., 2017. Sensory coding and cognitive processing of sound in Veterans with blast exposure. Hear Res 349, 98-110.

Brouwer, S., Bradlow, A.R., 2016. The Temporal Dynamics of Spoken Word Recognition in Adverse Listening Conditions. J Psycholinguist Res 45, 1151-1160.

Calderone, D.J., Lakatos, P., Butler, P.D., Castellanos, F.X., 2014. Entrainment of neural oscillations as a modifiable substrate of attention. Trends in Cognitive Sciences Trends in Cognitive Sciences 18, 300-309.

C□eponien, R., Cheour, M., Na□a□ta□nen, R., 1998. Interstimulus interval and auditory event-related potentials in children: evidence for multiple generators. Electroencephalography and Clinical Neurophysiology/Evoked Potentials Section Electroencephalography and Clinical Neurophysiology/Evoked Potentials Section 108, 345-354.

Choi, I., Kim, S., Choi, I., Schwalje, A., 2020. Cortical dynamics of speech-in-noise understanding. Acoust. Sci. Technol. Acoustical Science and Technology 41, 400-403.

Choi, I., Rajaram, S., Varghese, L.A., Shinn-Cunningham, B.G., 2013. Quantifying attentional modulation of auditory-evoked cortical responses from single-trial electroencephalography. Front Hum Neurosci 7, 115.

Choi, I., Wang, L., Bharadwaj, H., Shinn-Cunningham, B., 2014. Individual differences in attentional modulation of cortical responses correlate with selective attention performance. Hear Res 314, 10-19.

Dahan, D., Gareth Gaskell, M., 2007. The temporal dynamics of ambiguity resolution: Evidence from spoken-word recognition. J Mem Lang 57, 483-501.

Dahan, D., Magnuson, J.S., 2006. Spoken word recognition. Handbook of psycholinguistics. Elsevier, pp. 249-283.

Dai, L., Shinn-Cunningham, B.G., 2016. Contributions of sensory coding and attentional control to individual differences in performance in spatial auditory selective attention tasks. Front Hum Neurosci 10, 530.

Dai, L., Shinn-Cunningham, B.G., Best, V., 2018. Sensorineural hearing loss degrades behavioral and physiological measures of human spatial selective auditory attention. Proc.

696 Natl. Acad. Sci. U. S. A. Proceedings of the National Academy of Sciences of the United
697 States of America 115, E3286-E3295.
698 Dale, A.M., Liu, A.K., Fischl, B.R., Buckner, R.L., Belliveau, J.W., Lewine, J.D., Halgren, E.,
699 2000. Dynamic statistical parametric mapping: combining fMRI and MEG for high-resolution
700 imaging of cortical activity. Neuron 26, 55-67.
701 Darwin, C.J., 1997. Auditory grouping. Trends Cogn Sci 1, 327-333.
702 Davis, M.H., 2016. The Neurobiology of Lexical Access. Neurobiology of Language. Elsevier,
703 pp. 541-555.
704 Davis, M.H., Gaskell, M.G., 2009. A complementary systems account of word learning: neural
705 and behavioural evidence. Philosophical transactions of the Royal Society of London.
706 Series B, Biological sciences. 364, 3773.
707 Davis, M.H., Johnsrude, I.S., 2003. Hierarchical processing in spoken language comprehension.
708 The Journal of neuroscience : the official journal of the Society for Neuroscience 23, 3423-
709 3431.
710 Ding, N., Melloni, L., Zhang, H., Tian, X., Poeppel, D., 2016. Cortical tracking of hierarchical
711 linguistic structures in connected speech. Nat Neurosci Nature Neuroscience 19, 158-164.
712 Ding, N., Simon, J.Z., Chatterjee, M., 2014. Robust cortical entrainment to the speech envelope
713 relies on the spectro-temporal fine structure. NeuroImage NeuroImage 88, 41-46.
714 Du, Y., Buchsbaum, B.R., Grady, C.L., Alain, C., 2014. Noise differentially impacts phoneme
715 representations in the auditory and speech motor systems. Proc Natl Acad Sci U S A 111,
716 7126-7131.
717 Du, Y., Buchsbaum, B.R., Grady, C.L., Alain, C., 2016. Increased activity in frontal motor cortex
718 compensates impaired speech perception in older adults. Nat Commun 7, 12241.
719 Etard, O., Reichenbach, T., 2019. Neural Speech Tracking in the Theta and in the Delta
720 Frequency Band Differentially Encode Clarity and Comprehension of Speech in Noise. The
721 Journal of neuroscience : the official journal of the Society for Neuroscience 39, 5750-5759.
722 Farris-Trimble, A., McMurray, B., 2013. Test-retest reliability of eye tracking in the visual world
723 paradigm for the study of real-time spoken word recognition. Journal of Speech Language
724 and Hearing Research 56, 1328-1345.
725 Farris-Trimble, A., McMurray, B., Cigrand, N., Tomblin, J.B., 2014. The process of spoken word
726 recognition in the face of signal degradation. Journal of Experimental Psychology: Human
727 Perception and Performance Journal of Experimental Psychology: Human Perception and
728 Performance 40, 308-327.
729 Fischl, B., van der Kouwe, A., Destrieux, C., Halgren, E., Ségonne, F., Salat, D.H., Busa, E.,
730 Seidman, L.J., Goldstein, J., Kennedy, D., Caviness, V., Makris, N., Rosen, B., Dale, A.M.,
731 2004. Automatically parcellating the human cerebral cortex. Cereb Cortex 14, 11-22.
732 Frey, J.N., Mainy, N., Lachaux, J.P., Muller, N., Bertrand, O., Weisz, N., 2014. Selective
733 Modulation of Auditory Cortical Alpha Activity in an Audiovisual Spatial Attention Task.
734 JOURNAL OF NEUROSCIENCE 34, 6634.
735 Friston, K., Harrison, L., Daunizeau, J., Kiebel, S., Phillips, C., Trujillo-Barreto, N., Henson, R.,
736 Flandin, G., Mattout, J., 2008. Multiple sparse priors for the M/EEG inverse problem.
737 Neuroimage 39, 1104-1120.
738 Giraud, A.L., Poeppel, D., 2012. Cortical oscillations and speech processing: emerging
739 computational principles and operations. Nature neuroscience 15, 511-517.
740 Goldberg, H.R., Choi, I., Varghese, L.A., Bharadwaj, H., Shinn-Cunningham, B.G., 2014.
741 Auditory attention in a dynamic scene: Behavioral and electrophysiological correlates. The
742 Journal of the Acoustical Society of America The Journal of the Acoustical Society of
743 America 135, 2415.
744 Golumbic, E.M.Z., Ding, N., Bickel, S., Lakatos, P., Schevon, C.A., McKhann, G.M., Goodman,
745 R.R., Emerson, R., Mehta, A.D., Simon, J.Z., Poeppel, D., Schroeder, C.E., 2013.

Mechanisms Underlying Selective Neuronal Tracking of Attended Speech at a Cocktail Party. NEURON Neuron 77, 980-991.

Gow, D.W., Jr., 2012. The cortical organization of lexical knowledge: a dual lexicon model of spoken language processing. Brain Lang 121, 273-288.

Gramfort, A., Luessi, M., Larson, E., Engemann, D.A., Strohmeier, D., Brodbeck, C., Goj, R., Jas, M., Brooks, T., Parkkonen, L., Hamalainen, M., 2013. MEG and EEG data analysis with MNE-Python. Front Neurosci 7, 267.

Gramfort, A., Luessi, M., Larson, E., Engemann, D.A., Strohmeier, D., Brodbeck, C., Parkkonen, L., Hamalainen, M.S., 2014. MNE software for processing MEG and EEG data. Neuroimage 86, 446-460.

Hämäläinen, M.S., Sarvas, J., 1989. Realistic conductivity geometry model of the human head for interpretation of neuromagnetic data. IEEE Trans Biomed Eng 36, 165-171.

Harris, R.W., Swenson, D.W., 1990. Effects of reverberation and noise on speech recognition by adults with various amounts of sensorineural hearing impairment. Audiology 29, 314-321.

Herrmann, B.r., Henry, M.J., Haegens, S., Obleser, J., 2016. Temporal expectations and neural amplitude fluctuations in auditory cortex interactively influence perception. YNIMG NeuroImage 124, 487-497.

Hickok, G., Poeppel, D., 2007. The cortical organization of speech processing. Nat Rev Neurosci 8, 393-402.

Hillyard, S.A., Hink, R.F., Schwent, V.L., Picton, T.W., 1973. Electrical signs of selective attention in the human brain. Science 182, 177-180.

Hillyard, S.A., Vogel, E.K., Luck, S.J., 1998. Sensory gain control (amplification) as a mechanism of selective attention: electrophysiological and neuroimaging evidence. Philos Trans R Soc Lond B Biol Sci 353, 1257-1270.

Holmes, E., Griffiths, T.D., 2019. 'Normal' hearing thresholds and fundamental auditory grouping processes predict difficulties with speech-in-noise perception. Scientific reports 9.

Hornickel, J., Skoe, E., Nicol, T., Zecker, S., Kraus, N., 2009. Subcortical differentiation of stop consonants relates to reading and speech-in-noise perception. Proc Natl Acad Sci U S A 106, 13022-13027.

Huettig, F., Altmann, G.T., 2005. Word meaning and the control of eye fixation: semantic competitor effects and the visual world paradigm. Cognition 96, B23-32.

Kisler, T., Reichel, U.D., Sciel, F., 2017. Multilingual processing of speech via web services. Computer Speech & Language 45, 326-347.

Koessler, L., Maillard, L., Benhadid, A., Vignal, J.P., Felblinger, J., Vespignani, H., Braun, M., 2009. Automated cortical projection of EEG sensors: Anatomical correlation via the international 10-10 system. YNIMG NeuroImage 46, 64-72.

Kong, Y.Y., Somarowthu, A., Ding, N., 2015. Effects of Spectral Degradation on Attentional Modulation of Cortical Auditory Responses to Continuous Speech. JARO -NEW YORK- 16, 783-796.

Lange, K., 2009. Brain correlates of early auditory processing are attenuated by expectations for time and pitch. Brain and cognition. 69, 127.

Lee, A.K.C., Rajaram, S., Xia, J., Bharadwaj, H., Larson, E., Hämäläinen, M.S., Shinn-Cunningham, B.G., 2013. Auditory Selective Attention Reveals Preparatory Activity in Different Cortical Regions for Selection Based on Source Location and Source Pitch. Front. Neurosci. Frontiers in Neuroscience 6, 190.

Liberman, M.C., Epstein, M.J., Cleveland, S.S., Wang, H., Maison, S.F., 2016. Toward a differential diagnosis of hidden hearing loss in humans. PLoS One 11, 1-16.

Luck, S.J., 2014. An introduction to the event-related potential technique, Second edition. ed. The MIT Press, Cambridge, Massachusetts.

796 Magnuson, J.S., Dixon, J.A., Tanenhaus, M.K., Aslin, R.N., 2007. The dynamics of lexical
797 competition during spoken word recognition. Cogn Sci 31, 133-156.
798 Maris, E., Oostenveld, R., 2007. Nonparametric statistical testing of EEG- and MEG-data. J
799 Neurosci Methods 164, 177-190.
800 McMurray, B., Ellis, T.P., Apfelbaum, K.S., 2019. How Do You Deal With Uncertainty? Cochlear
801 Implant Users Differ in the Dynamics of Lexical Processing of Noncanonical Inputs. Ear and
802 hearing 40, 961-980.
803 McMurray, B., Farris-Trimble, A., Rigler, H., 2017. Waiting for lexical access: Cochlear implants
804 or severely degraded input lead listeners to process speech less incrementally. Cognition
805 169, 147-164.
806 McMurray, B., Samelson, V.M., Lee, S.H., Bruce Tomblin, J., 2010. Individual differences in
807 online spoken word recognition: Implications for SLI. Cognitive Psychology Cognitive
808 Psychology 60, 1-39.
809 McQueen, J.M., Huettig, F., 2012. Changing only the probability that spoken words will be
810 distorted changes how they are recognized. The Journal of the Acoustical Society of
811 America The Journal of the Acoustical Society of America 131, 509-517.
812 Mesgarani, N., Chang, E.F., 2012. Selective cortical representation of attended speaker in multi-
813 talker speech perception. Nature 485, 233-236.
814 Moore, B.C., 1990. Co-modulation masking release: spectro-temporal pattern analysis in
815 hearing. British journal of audiology 24, 131-137.
816 Myers, E.B., Blumstein, S.E., Walsh, E., Eliassen, J., 2009. Inferior Frontal Regions Underlie the
817 Perception of Phonetic Category Invariance. PSCI Psychological Science 20, 895-903.
818 Nabelek, A.K., 1988. Identification of vowels in quiet, noise, and reverberation: relationships
819 with age and hearing loss. J Acoust Soc Am 84, 476-484.
820 O'Sullivan, J., Mesgarani, N., Smith, E., Schevon, C., McKhann, G.M., Sheth, S.A., Herrero, J.,
821 Mehta, A.D., Smith, E., Sheth, S.A., 2019. Hierarchical Encoding of Attended Auditory
822 Objects in Multi-talker Speech Perception. NEURON Neuron 104, 1195-1209.e1193.
823 Obleser, J., Erb, J., 2020. Neural Filters for Challenging Listening Situations. The Cognitive
824 Neurosciences. MIT Press.
825 Obleser, J., Kayser, C., 2019. Neural Entrainment and Attentional Selection in the Listening
826 Brain. Trends Cogn Sci 23, 913-926.
827 Ohlenforst, B., Zekveld, A.A., Lunner, T., Wendt, D., Naylor, G., Wang, Y., Versfeld, N.J.,
828 Kramer, S.E., 2017. Impact of stimulus-related factors and hearing impairment on listening
829 effort as indicated by pupil dilation. Hear Res 351, 68-79.
830 Owens, E., Schubert, E.D., 1977. Development of the California Consonant Test. J Speech
831 Lang Hear Res. 20, 463-474.
832 Parbery-Clark, A., Skoe, E., Kraus, N., 2009. Musical experience limits the degradative effects
833 of background noise on the neural processing of sound. J Neurosci 29, 14100-14107.
834 Pelli, D.G., 1997. The VideoToolbox software for visual psychophysics: transforming numbers
835 into movies. Spat Vis 10, 437-442.
836 Rauschecker, J.P., Scott, S.K., 2009. Maps and streams in the auditory cortex: nonhuman
837 primates illuminate human speech processing. Nature neuroscience 12, 718-724.
838 Rigler, H., Farris-Trimble, A., Greiner, L., Walker, J., Tomblin, J.B., McMurray, B., 2015. The
839 slow developmental timecourse of real-time spoken word recognition. Developmental
840 psychology 51, 1690-1703.
841 Scott, S.K., Johnsrude, I.S., 2003. The neuroanatomical and functional organization of speech
842 perception. Trends Neurosci 26, 100-107.
843 Shamma, S., Elhilali, M., Ma, L., Micheyl, C., Oxenham, A.J., Pressnitzer, D., Yin, P., Xu, Y.,
844 2013. Temporal coherence and the streaming of complex sounds. Advances in
845 experimental medicine and biology 787, 535-543.

Shinn-Cunningham, B.G., 2020. 14 Brain Mechanisms of Auditory Scene Analysis. The Cognitive Neurosciences, pp. 159-166.

Shinn-Cunningham, B.G., Best, V., 2008. Selective attention in normal and impaired hearing. Trends Amplif 12, 283-299.

Song, J.H., Skoe, E., Banai, K., Kraus, N., 2011. Perception of Speech in Noise: Neural Correlates. Journal of Cognitive Neuroscience 23, 2268-2279.

Strait, D.L., Kraus, N., 2011. Can you hear me now? Musical training shapes functional brain networks for selective auditory attention and hearing speech in noise. Frontiers in psychology 2, 113-113.

Strauss, D.J., Francis, A.L., 2017. Toward a taxonomic model of attention in effortful listening. Cognitive, Affective, & Behavioral Neuroscience 17, 809-825.

Taylor, J.S.H., Rastle, K., Davis, M.H., 2013. Can Cognitive Models Explain Brain Activation During Word and Pseudoword Reading? A Meta-Analysis of 36 Neuroimaging Studies. PSYCHOLOGICAL BULLETIN 139, 766-791.

Teki, S., Kumar, S., Von Kriegstein, K., Griffiths, T.D., Chait, M., 2011. Brain bases for auditory stimulus-driven figure-ground segregation. J. Neurosci. Journal of Neuroscience 31, 164-171.

Tong, Y., Chen, Q., Nichols, T.E., Rasetti, R., Callicott, J.H., Berman, K.F., Weinberger, D.R., Mattay, V.S., 2016. Seeking optimal region-of-interest (ROI) single-value summary measures for fMRI studies in imaging genetics. PLoS One 11, 1-20.

Tune, S., Alavash, M., Fiedler, L., Obleser, J., 2020. Neural attention filters do not predict behavioral success in a large cohort of aging listeners. bioRxiv, 2020.2005.2020.105874.

Vaden, K.I., Jr., Kuchinsky, S.E., Ahlstrom, J.B., Dubno, J.R., Eckert, M.A., 2015. Cortical activity predicts which older adults recognize speech in noise and when. J Neurosci 35, 3929-3937.

Viswanathan, V., Bharadwaj, H.M., Shinn-Cunningham, B.G., 2019. Electroencephalographic Signatures of the Neural Representation of Speech during Selective Attention. eNeuro 6.

Weber, A., Scharenborg, O., 2012. Models of spoken-word recognition Models of word recognition. WIREs Cogn Sci Wiley Interdisciplinary Reviews: Cognitive Science 3, 387-401.

Wong, P.C., Jin, J.X., Gunasekera, G.M., Abel, R., Lee, E.R., Dhar, S., 2009. Aging and cortical mechanisms of speech perception in noise. Neuropsychologia 47, 693-703.

Wong, P.C., Uppunda, A.K., Parrish, T.B., Dhar, S., 2008. Cortical mechanisms of speech perception in noise. J Speech Lang Hear Res 51, 1026-1041.

Zekveld, A.A., Heslenfeld, D.J., Festen, J.M., Schoonhoven, R., 2006. Top-down and bottom-up processes in speech comprehension. Neuroimage 32, 1826-1836.

884 **Figure Legends**

885 **Figure 1.** Trial and stimulus structure. Every trial starts with the cue phrase "check the word." A
886 target word starts 1 second after the noise onset. Four choices are given after the word ends;
887 subjects select the correct answer with a keypad. No feedback is given. The noise level is
888 manipulated to create high (+3 dB) and low (-3 dB) SNR conditions. Subjects complete 50 trials
889 for each condition.
890

891 **Figure 2.** Behavioral results. **A.** Summary of behavioral performance for the two conditions (+3
892 and -3 dB SNR). Boxes denote the 25^{th} – 75^{th} percentile range; the horizontal bars in the center
893 denote the median; the ranges are indicated by vertical dashed lines. Solid lines connect points
894 for the same subject in different conditions. **B.** Average accuracy as a function of reaction time
895 in +3 dB SNR condition. **C.** Average accuracy and reaction time in -3 dB SNR condition.
896

897 **Figure 3.** Sensor-level event-related potential (ERP) with the topographical layout and cortical
898 maps. The time course of the auditory ERP and its envelope, with the standard error of the
899 mean (±1 SEM) at the peak amplitude (red color: +3 dB SNR, blue color: -3 dB SNR). An
900 asterisk shows a significant difference in the amplitude between +3 and -3 dB SNR conditions
901 (paired *t*-test). Top panels show peak P2 amplitudes of all electrodes in topographical layouts.
902 The *t*-values from paired *t*-tests between two SNR conditions are also shown as topographies.
903

904 **Figure 4**. Region-of-interest (ROI) based source analysis. **A and B.** The time course of the
905 event-related potential (ERP) envelope, with the standard error of the mean (±1 SEM), obtained
906 at representative voxels for two ROIs in the left hemisphere ("LH"): supramarginal gyrus (SMG),
907 and the pars opercularis and triangularis of the inferior frontal gyrus (IFG), respectively, in each
908 SNR condition (red color: +3 dB SNR, blue color: -3 dB SNR). The ERP envelope time courses
909 in the corresponding regions in the right hemisphere ("RH") are also shown for visual
910 comparisons. Asterisks show the timing of a significant difference between +3 and -3 dB SNR
911 conditions (cluster-based permutation test, $p = 0.0020$) at the left SMG. **C and D.** Whole-brain
912 maps showing statistical contrasts (*t*-values obtained from post-hoc paired *t*-tests between the
913 two SNR conditions) of source activation at each voxel at the peak timepoint of the grand-
914 average source time course of each ROI.
915

916 **Figure 5.** Top and second panel show histograms of boundaries between phonemes of each
917 stimulus. The third panel shows superimposed temporal envelopes extracted from waveforms of
918 the 100 words.
919

920 **Figure 6.** Individual differences in speech-in-noise processing. **A**. Regression coefficients and
921 their standard errors. **B**. A scatter plot showing the relationship between predicted and
922 measured accuracy in -3 dB SNR condition. **C**. Post-hoc correlation analyses: Raw correlations
923 between each independent variable and the dependent variable. **D**. Left: Relationship between
924 independent variables shows no correlation between internal SNR and evoked source current at
925 the left supramarginal gyrus (SMG). Right: Semi-partial correlation between SMG evoked
926 source current and the residual of accuracy after regressing out internal SNR. **E**. The time
927 course of the auditory event-related potential and its envelope, with the standard error of the
928 mean (±1 SEM) at the peak magnitude in -3 dB SNR condition (red color: good performers, blue

929 color: poor performers). An asterisk shows a significant difference in the magnitude between
930 two groups (two-sample *t*-test).
931